

Arrangement of Phases of Double-circuit Three-phase Overhead Power Lines and Its Influence on Buried Parallel Equipment

Lenka Šroubová¹⁾, Roman Hamar²⁾ and Petr Kropík³⁾

University of West Bohemia / Department of Theory of Electrical Engineering, Plzeň, Czech Republic

e-mail: ¹⁾ lsroubov@kte.zcu.cz, ²⁾ hamar@kte.zcu.cz, ³⁾ pkropik@kte.zcu.cz

Abstract — This paper deals with electromagnetic fields around double-circuit three-phase overhead power lines and their interference effects on the buried parallel equipment, such as pipelines or cables. The paper provides both an analysis of electric and magnetic fields around double-circuit power transmission lines and a simulation of how these fields influence buried equipment.

Keywords — Double-circuit transmission line, electric and magnetic fields around overhead lines.

I. INTRODUCTION

Transmission lines (vhv, hv) for transferring very high power are usually designed as double-circuit three-phase overhead lines with earth wires. Due to the proximity of both circuits, their mutual effects have to be considered. To reduce the mutual interference, the overhead lines are usually transposed. With respect to the position of the phase conductors, the transposition is not always equally efficient. Besides positive effects on the impedance of the line, the optimised arrangement of the conductors can reduce the electric and magnetic field strengths in their vicinity and, consequently, their negative impact on the environment. The maximum safe values of both the electric and magnetic field strengths with respect to their effects on human bodies are stipulated by safety regulations. The optimised transposition enables a better satisfaction of these requirements [14]. The analysis was carried out by the professional software MATLAB [13] with a number of special in-house scripts.

At present, there is a tendency towards building power corridors for more transmission systems. The reasons are difficulties in getting sites, high cost of land, environment protection, etc. Particular systems, however, may influence one another. The paper deals with the influence of an overhead line on a buried pipeline, too. These problems are geometrically incommensurable (i.e. the diameter of a pipeline versus the distance between conductors of an overhead line and land surface). The problem was solved using the simulation software Agros2D [12] and COMSOL Multiphysics [11] supplemented with a number of special in-house scripts.

II. MATHEMATICAL MODEL

A. Analytical Solution of the Problem

Let us consider a double-circuit overhead line with two earth wires as shown in Fig. 1. On condition that voltage and current systems are balanced, the currents in the earth

wires are negligible and voltages between the earth wires and earth are equal to zero. Supposing sinusoidal steady state, the complex representation of time varying functions can be used. If the phases a_1, b_1, c_1 in circuit No. 1 are placed on the conductors 1, 2, and 3, and the phases a_2, b_2, c_2 in circuit No. 2 are placed on the conductors 5, 6 and 7, then the voltage and current phasors can be expressed in the matrix forms

$$\mathbf{U}_1 = U_1 \begin{bmatrix} 1 \\ \mathbf{a}^2 \\ \mathbf{a} \end{bmatrix} \quad \mathbf{I}_1 = I_1 \begin{bmatrix} 1 \\ \mathbf{a}^2 \\ \mathbf{a} \end{bmatrix} \quad (1)$$

where U_1 and I_1 are amplitudes of the phase voltage and current in the circuit No. 1 and $\mathbf{a} = e^{2\pi/3}$. There are thirty-six possible arrangements of the phases in the layout but only six of them are basic. The other arrangements provide the same results. These six basic arrangements of the phases can be defined in terms of the columns \mathbf{p}_i of the matrix \mathbf{P}

$$\mathbf{P} = \{\mathbf{p}_1, \mathbf{p}_2, \mathbf{p}_3, \mathbf{p}_4, \mathbf{p}_5, \mathbf{p}_6\} = \begin{bmatrix} 1 & 1 & \mathbf{a} & \mathbf{a}^2 & \mathbf{a}^2 & \mathbf{a} \\ \mathbf{a}^2 & \mathbf{a} & 1 & 1 & \mathbf{a} & \mathbf{a}^2 \\ \mathbf{a} & \mathbf{a}^2 & \mathbf{a}^2 & \mathbf{a} & 1 & 1 \end{bmatrix}. \quad (2)$$

If the arrangement of the phases in the circuit No.1 is given by the column \mathbf{p}_i and in the circuit No. 2 by the column \mathbf{p}_j respectively, the matrices of voltage and current phasors are

$$\mathbf{I}_{ij} = \begin{bmatrix} I_1 \mathbf{p}_i \\ I_2 \mathbf{p}_j \end{bmatrix} \quad (3)$$

$$\mathbf{U}_{ij} = \begin{bmatrix} U_1 \mathbf{p}_i \\ U_2 \mathbf{p}_j \end{bmatrix} \quad (4)$$

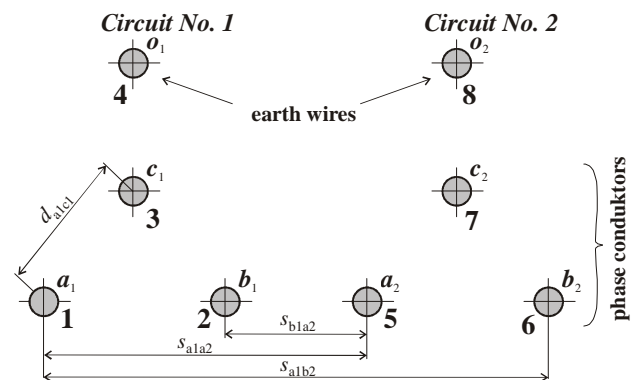


Fig. 1. Conductors of a double-circuit overhead line.

It is well-known that the electric field strength of one conductor above the perfectly conducting earth – see Fig. 2 – is proportional to the magnitude of its charge (which is given by Eq. (6)) and to the distances r_{ij} , r'_{ij} (given by the layout of the conductor and its projection and by the position of the point M at which the electric field strength is calculated).

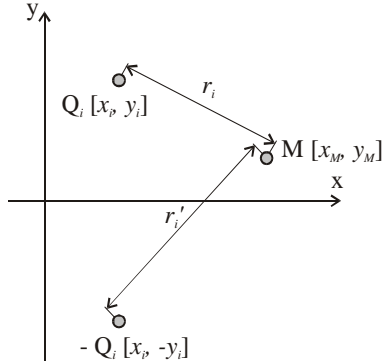


Fig. 2. Calculation of electric strength at point M.

For the x and y the phasor components of the electric field strength we obtain

$$\begin{aligned} E_{xi}(M) &= kQ_i D_{xi} \\ E_{yi}(M) &= kQ_i D_{yi} \end{aligned} \quad (5)$$

$$i, j = 1, 2, \dots, 8$$

where

$$D_{xi} = (x_M - x_i) \left(\frac{1}{r_i^2} - \frac{1}{r_i'^2} \right)$$

$$D_{yi} = \frac{y_i - y_M}{r_i^2} + \frac{y_i + y_M}{r_i'^2}$$

$$r_i = \sqrt{(x_M - x_i)^2 + (y_M - y_i)^2}$$

$$r_i' = \sqrt{(x_M - x_i)^2 + (y_M + y_i)^2}$$

and Q is the charge of the conductor.

The matrix of the conductor charges for a known phase voltage can be determined by means of the method of partial capacitances. After expressing the matrix of the potential coefficients \mathbf{A} , we can find the inverse matrix \mathbf{B} .

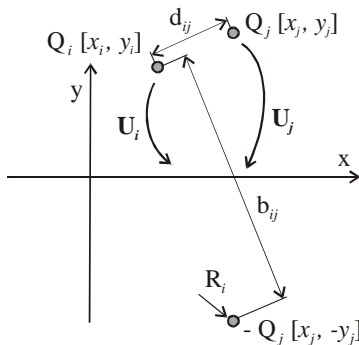


Fig. 3. Calculation of capacitance coefficients (matrix \mathbf{B})

The charges on each conductor of a double-circuit line for any arrangement of the phases (circuit No.1 according to the column \mathbf{p}_i and circuit No. 2 according to the column \mathbf{p}_j) are given by the matrix \mathbf{Q}_i elements j

$$\mathbf{Q}_{ij}(8,1) = \begin{bmatrix} U_1 \mathbf{B}_{11} \mathbf{p}_i + U_2 \mathbf{B}_{12} \mathbf{p}_j \\ U_1 \mathbf{B}_{21} \mathbf{p}_i + U_2 \mathbf{B}_{22} \mathbf{p}_j \end{bmatrix} \quad (6)$$

where the submatrix \mathbf{B}_{11} of the matrix \mathbf{B} respects the mutual capacitance effects in the circuit No. 1 and \mathbf{B}_{12} expressing the impact of the circuit No. 2 on the circuit No. 1. The situation is similar for the submatrices \mathbf{B}_{21} and \mathbf{B}_{22} (see [5] for more details).

After superposition, we receive the magnitude of the resultant electric field strength at the point M:

$$E_{xM} = \sum_i E_{xi}(M) \quad E_{yM} = \sum_i E_{yi}(M) \quad E_M = \sqrt{|E_{xM}|^2 + |E_{yM}|^2} \quad (7)$$

The x and y components of the phasor of the magnetic field strength at the point M which are produced by the current of the i -th conductor (see Eq. (3)) are given by the following formulae

$$H_{xi}(M) = \frac{I_i}{2\pi} \frac{y_i - y_M}{r_i^2} \quad H_{yi}(M) = \frac{I_i}{2\pi} \frac{x_M - x_i}{r_i^2} \quad (8)$$

where $r_i = \sqrt{(x_M - x_i)^2 + (y_M - y_i)^2}$, $i, j = 1, 2, \dots, 8$.

The problem was solved using the professional software MATLAB [12] supplemented with a number of special in-house scripts. These scripts provide the ability to set parameters of the computations for different types of towers, various voltages, currents and their phase shifts, arrangement of phases, and for conductors' sags. Any height of conductors above the earth's surface and a span of tower can be chosen for the computation of the electric and magnetic fields. The electric and magnetic fields can be calculated at any height above the earth. The user can set its own configuration. Our scripts allow automating the evaluation process, for example in given intervals, using preset steps, etc.

The correctness of the analytical solution was verified by a numerical solution using the simulation software Agros2D [11] and COMSOL Multiphysics [10].

B. The Model and Area of Numerical Computation

The aim was not only to solve the magnetic field distribution around overhead lines, but also its influence on buried pipelines.

In fact, buried pipelines are hardly ever arranged in parallel with the double-circuit overhead lines. Often they only cross the corridor at some angle or even perpendicularly. In such cases, however, the influence of the overhead line on the pipeline is lower and will not be dealt with here.

The concerned values of the magnetic field are also influenced by the conductor sags. For the same reason, computations are performed for the given height of the conductors above the ground.

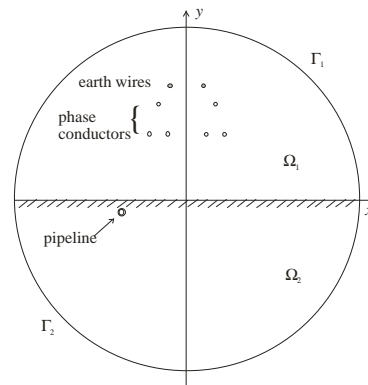


Fig. 4. The area for numerical computation.

The investigated domain is considered linear (i.e., even the steel pipeline is supposed to exhibit a constant permeability, which is possible due to its rather low saturation). In the steady state, the electromagnetic field generated by the overhead line is then harmonic and may be described by the Helmholtz equation for the z -th component of the magnetic vector potential A phasor

$$\Delta \underline{A} - j\omega\gamma\mu \underline{A} = \mu \underline{J}_{\text{ext}} \quad (9)$$

The problem is solved two-dimensionally in the Cartesian coordinate system x, y , as the model does not change in the direction of the z -axis.

$$\Delta \underline{A}_z - j\omega\gamma\mu \underline{A}_z = \mu \underline{J}_{\text{ext},z} \quad (10)$$

where $\underline{J}_{\text{ext},z}$ is the z -th component of the external current density phasor in the conductors of the overhead line, μ denotes the magnetic permeability, γ stands for the electric conductivity, and ω is the angular frequency.

The two-dimensional area Ω is defined. This area Ω consists of two main subareas Ω_1 (air), Ω_2 (soil) (see Fig. 4). The pipeline in soil with the other considered subareas is depicted in Fig 5. Eq. (10) is applied to each of the areas separately [1].

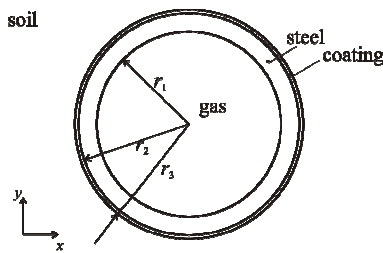


Fig. 5. Example of a buried pipeline.

The time-average volumetric value of heat generated by resistive heating of the steel pipeline is then given by the expression

$$Q_{\text{av}} = \frac{1}{2} \text{Re} \left\{ \frac{\underline{J}_z \cdot \underline{J}_z}{\gamma} \right\} \quad (11)$$

where \underline{J}_z denotes the total current density in the pipeline.

The computations were performed by Agros2D [12] and COMSOL Multiphysics [11] supplemented with a number of special in-house procedures. The paper compares the results obtained from these two software applications.

III. ILLUSTRATIVE EXAMPLE

The analysis of the electric and magnetic field was performed for a double-circuit tower of the “Donau” type carrying two parallel overhead lines.

Supposing the overhead line ended with the surge impedance loading, the magnitude of the current is given by the real power and rated voltage:

$$U_1 = U_2 = 400 \text{ [kV]}, \quad I_1 = I_2 = 790 \text{ [A]}.$$

The distribution of the field at a height of 1.2 m above the earth was calculated for six basic arrangements (given by the matrix \mathbf{P} – Eq. (2)), and for the distance given by the size of the tower. The observed values are higher with the conductor sags.

TABLE I.
ARRANGEMENT OF THE PHASES

Phase Arrangement	Curve Number
$\begin{matrix} \times & \times \\ \bullet & \circ \end{matrix}$	1
$\begin{matrix} \circ & \times \\ \bullet & \bullet \end{matrix}$	2
$\begin{matrix} \times & \times \\ \circ & \bullet \end{matrix}$	3
$\begin{matrix} \bullet & \times \\ \circ & \bullet \end{matrix}$	4
$\begin{matrix} \circ & \times \\ \times & \bullet \end{matrix}$	5
$\begin{matrix} \bullet & \times \\ \times & \circ \end{matrix}$	6

We investigated the situation for six basic transpositions of the overhead line according to Table 1. The arrangement of the phases is marked by the symbols „•“, „◦“ and „×“.

The distribution of E [kV/m] and B [μT] is depicted in Fig. 6. The numbers of curves correspond to the arrangement of the phase conductors, as shown in Tab 1, 2nd column.

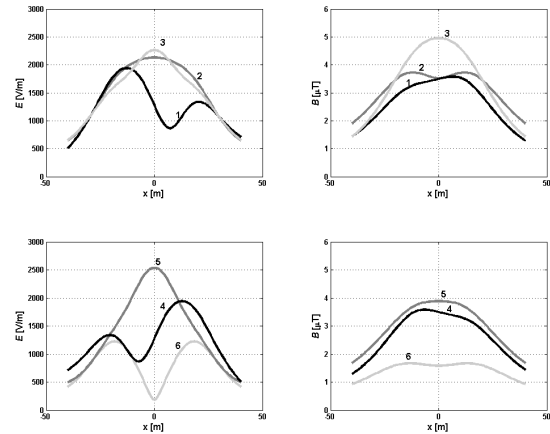


Fig. 6. Distribution of E [kV/m] and B [μT] for the “Donau” type tower. The curves numbers correspond to the phase arrangement (Tab. 1).

The first example shows that an optimum arrangement is achieved when the conductors of the same phases are separated as much as possible from each other and the distance between the different phases is kept as small as possible.

Conversely, an undesirable arrangement occurs if the phases are placed symmetrically, enantiomorphly or the conductors of the same phase are close to one another. In those cases the magnetic field is twice or three-times higher than in the optimum case. The allowable value of the electric field strength is 5 kV/m and the allowable value of the magnetic flux density is 100 μT [11]. The results clearly indicate that the Donau tower exceeded the allowable value in places where the conductors were located at a minimal height above the ground.

In the following example, the subject of this study is a steel pipeline. The conductivity of steel roughly ranges from 10^4 S/m to 10^6 S/m, in our case we consider $\gamma = 60000$ S/m. Its relative permeability is $\mu_r = 8000$. The gas in the pipeline is characterized by parameters $\gamma = 0$ and $\mu_r = 1$.

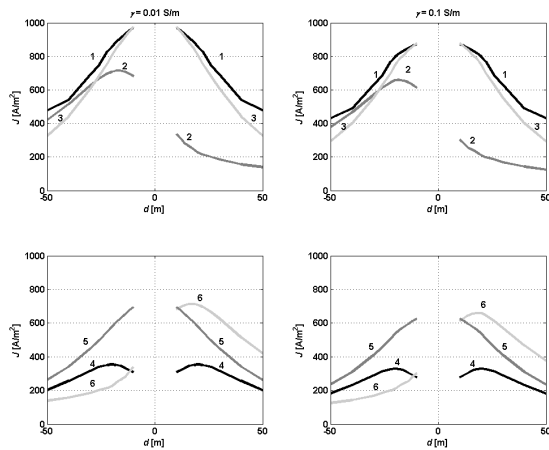


Fig. 7. The current density in the pipeline depending on the distance. The curves numbers correspond to the phase arrangement (Tab. 1).

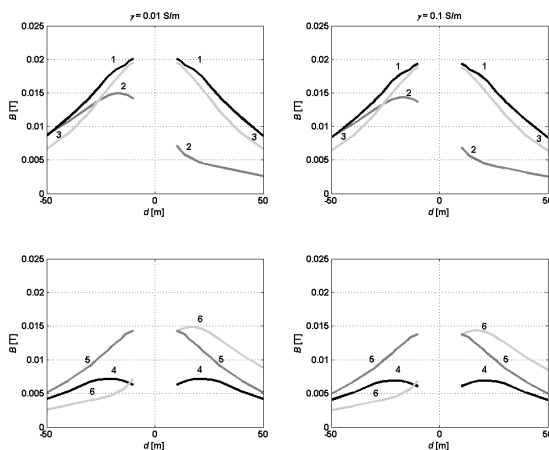


Fig. 8. The magnetic induction in the pipeline depending on the distance. The curves numbers correspond to the phase arrangement (Tab. 1).

The inner diameter of the pipeline is 0.5 m and its thickness is 0.02 m ($r_1 = 0.25$ m, $r_2 = 0.27$ m; see Fig. 2).

The steel pipeline is covered with an insulation coating. This coating mainly functions as corrosion protection, preventing the pipeline from direct contact with soil. The insulation is usually made of tar, asphalt, pitch, and cement and there are also advanced polymer coatings (made of polyethylene, polypropylene, etc.). Asphalt coatings are several mm to cm thick, but the thickness of polymer coatings is measured in μm . The insulation coating is characterized by the parameters $\gamma = 0$ and $\mu_r = 1$. Some cases it have also been solved for uncoated pipelines, or non-defective coatings, which do not affect the field distribution.

In practice, there is a change in soil type both vertically and horizontally; therefore, there is also a change in its conductivity γ . Moreover, the changes in the conductivity of soil depend not only on the soil type, but also on pH of soil, yearly rainfall and the level of ground water. Its values may range from 0.0005 S/m to 0.5 S/m. We chose a typical electric conductivity $\gamma = 0.01$ S/m and $\gamma = 0.1$ S/m for this illustrative example.

The computations were performed using the programs Agros2D [12] and COMSOL Multiphysics [11] supplemented with a number of special in-house scripts.

Another example shows a pipeline buried in parallel with a power overhead line suspended from a Donau tower (see Fig. 4).

The arrangement of the conductor phases has a significant effect on the situation in the pipeline. If we consider pipelines buried in parallel with two parallel lines, transposition affects the distribution of magnetic field in the vicinity of the lines and of course in the pipeline, too.

The influence of the phase conductor arrangement on the current density and magnetic induction in the pipeline in dependence on the distance from the tower is depicted in Fig. 7 and Fig. 8. The influence is studied at a distance of 10–50 m from the tower axis. The numbers of curves correspond to the arrangement of the phase conductors, as shown in Tab. 1. The observed values indicate that symmetrical or mirror arrangements are unsuitable.

Most of the observed current density values in the steel pipeline are higher than 100 A/m^2 (see Fig. 7), making the AC corrosion highly probable [15].

Fig. 7 and Fig. 8 show current density and magnetic induction, on the left side for the conductivity $\gamma = 0.01$ S/m, on the right side for $\gamma = 0.1$ S/m.

In the third example, we calculated the volumetric losses Q_{av} in the pipeline as functions of the distance d for particular arrangements listed in Tab. 1. The results are shown in Fig. 9.

A transposition in the double-circuit three-phase overhead lines has a considerable influence on the volumetric losses Q_{av} in the pipeline, too.

The highest volumetric losses in the pipeline during the normal operation occur in the variants when the phases are placed symmetrically with respect to the tower axis (variant 3 in Tab. 1).

This configuration is also the least favorable from the viewpoint of magnetic flux density penetrating the pipeline. The variant 5 is one of the negative variants. The variants 3 and 5 have the same phase closest to the tower axis.

The fourth example deals with the influence of an overhead line on a buried cable. However, as the conditions in the steel covering of the cable are significantly influenced by the magnetic field of the cable itself, we first investigated the situation in the cable covering without the influence of the overhead power lines. The volumetric heat losses are in W/m^3 again.

The three-phase power cable (Fig. 10) is buried in a depth of 1 m. The effective value of its nominal current is 100 A, voltage 10 kV and frequency 50 Hz.

The physical properties of copper are $\gamma = 5.8 \times 10^7$ S/m; relative permeability is $\mu_r = 1$. The insulation materials are characterized by the parameters $\gamma = 0$ and $\mu_r = 1$. The conductivity of soil is $\gamma = 0.01$ S/m and its relative permeability is $\mu_r = 1$, as in the previous example.

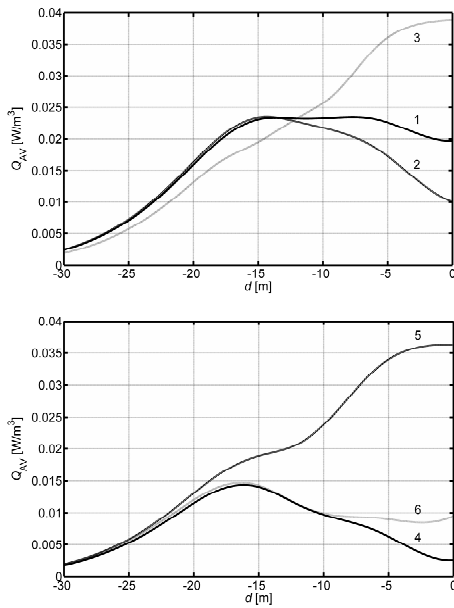


Fig. 9. Dependences of volumetric losses Q_{AV} in the pipeline on the distance d for the cases listed in Tab. 1.

The distance between the outmost conductor and the tower axis is 14.5 m. The distance between the center of the cable and tower axis lies between 0 to 30 m.

The dependences of the volumetric losses Q_{av} in the cable covering on the distance d for the arrangements listed in Tab. 1 are depicted in Fig. 11.

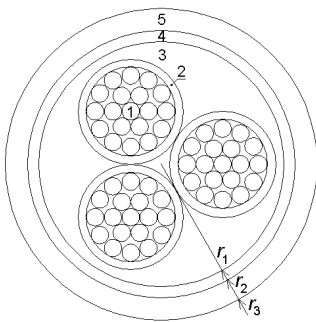


Fig. 10. Three-phase power cable: 1 – copper conductors, 2 – PVC insulation, 3 – rubber, 4 – steel covering (flat steel bands), 5 – outer PVC housing ($r_1 = 0.055$ m, $r_2 = 0.06$ m, $r_3 = 0.07$ m).

The computations are performed numerically, applying the finite element method. In addition, the methods of adaptivity were used. The code Agros2D enables the use of three types of adaptivity. The h -adaptivity is based on the division of an element into several smaller elements. The sizes or numbers of elements vary, while the polynomial orders of approximated quantities in the elements remain the same in the process. The p -adaptivity enlarges the orders of corresponding approximating polynomials, with the size of each element remaining the same. The hp -adaptivity represents the most complicated method. It is a combination of both above-mentioned methods; however, it is significantly different from both the h - and p -adaptivities.

This problem is geometrically incommensurable. On one hand, there is the field surrounding the outer double-circuit power overhead line (along tens to hundreds of meters), but on the other hand, there is the field in the buried pipeline (with a thickness of 0.02 m).

The h -adaptivity does not appear to be the best possible technique for the solution due to the geometrical incommensurability of the problem. The increase in the number of mesh elements leads to high requirements on computing power and available memory size. Therefore, it is better to solve this problem by increasing the order of approximating polynomials (i.e. by applying the p -adaptivity). The mesh remains unchanged in this case.

Fig. 12 compares the adaptive techniques implemented in Agros2D. It shows the dependence of the relative error of computations on the number of degrees of freedom.

The numerical solution to these problems was carried out using the software COMSOL Multiphysics [12]. The problem could have been solved only using the h -adaptive method in COMSOL because an increase in the number of mesh elements would not have led to a solution due to insufficient memory.

These examples were computed using the standard finite element method, but less accurately due to the number of degrees of freedom. The orders of the polynomials could have been increased, but only in particular domains. The computation was performed with these parameters:

- number of degrees of freedom: 169299,
- number of mesh points: 42378,
- order of polynomial: 2.

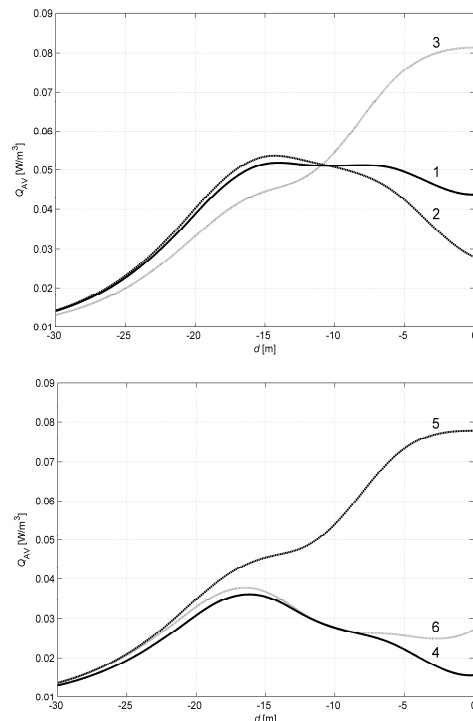


Fig. 11. Dependences of the volumetric losses Q_{av} in the cable covering on the distance d for arrangements listed in Tab. 1.

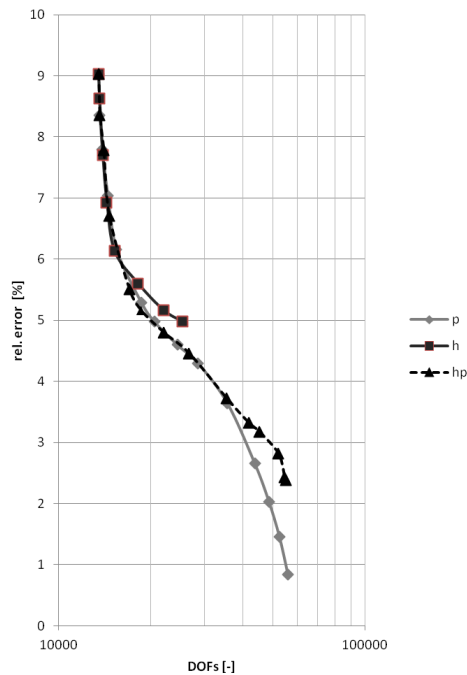


Fig. 12. Comparison of adaptive techniques.

IV. CONCLUSION

The results prove that the suitable arrangement of the phases of particular conductors leads to reduction of the magnetic field, namely in locations where the magnetic field can negatively affect the human body. The suggested algorithm can be used for double-circuit overhead lines with the same voltage level or for parallel lines with different voltage levels.

The values of the field distribution and the value of volumetric losses in buried parallel equipment are influenced by the distance of the buried parallel equipment from the overhead line, and by the conductivity of soil, which is variable both vertically and horizontally, depending on the soil composition. The value of the investigated volumetric losses is significantly influenced by the arrangement of phases in two parallel lines. The research shows that it is possible to find an optimal transposition of phase conductors, so that the value of the volumetric losses in the pipeline is minimized. The concerned value is also non-negligibly influenced by the conductor sags.

The software Agros2D with adaptivity converges to the solutions faster, and therefore the usage of Agros2D is effective. The method of the p -adaptivity is the most suitable in terms of speed for both presented examples and other examples of this type.

The buried parallel equipment and overhead lines can induce a field which may influence technical installations placed in the same corridor. The risks arise from the influence of high, extra high and ultra high voltage on metal pipes, especially the risk of damage to pipelines and the equipment associated with pipelines. Safety of all people working with this equipment and protection of other living organisms dwelling in this area must be ensured.

ACKNOWLEDGMENT

Financial support of project SGS-2015-035 is highly acknowledged.

REFERENCES

- [1] Šroubová, L., Hamar, R., Kropík, P. and Voráček, L. "Steel Buried Pipeline Influenced Power Overhead Line," in: *ELEKTRO 2012*. Žilina, University of Žilina, 2012, pp. 475 – 478, ISBN 978-1-4673-1178-6
- [2] Šroubová, L., Hamar, R. and Kropík, P. "Heating of Metal Covering of Buried Cable by Electromagnetic Effects of Power Overhead Line," in: *XXXV Miedzynarodowa konferencja z podstaw elektrotechniki i teorii obwodow*. Gliwice, Politechnika Slaska, 2012, pp. 45 – 46, ISBN: 978-83-85490-34-0.
- [3] Šroubová, L., Hamar, R., Kropík, P. "The Influence of Overhead Lines on Buried Cables," in *AMTEE '11 Proceedings*, University of West Bohemia, Pilsen, 2011, pp. II-25 – II-26
- [4] Benešová, Z., Šroubová, L., Mühlbacher, J. "Reduction of electric and magnetic field of double-circuit overhead lines," in *Komunalna energetika – Power engineering*, Maribor: Univerza v Mariboru, 2007, pp. 1 – 7.
- [5] Benešová, Z., Šroubová, L. "Reduction Electric and Magnetic Field of Double-Circuit Overhead Lines," in *AMTEE '03 Proceedings*, University of West Bohemia, Pilsen, 2003, pp. B1-B6.
- [6] Bortels, L., Deconinck, J., Munteanu, C., Topa, V. "A General Applicable Model for AC Predictive and Mitigation Techniques for Pipeline Networks Influenced by HV Power Lines," *IEEE Transactions on Power Delivery*, Vol. 21, No. 1, January 2006, pp. 210 – 217.
- [7] Christoforidis, G. C., Labridis, D. P., Dokopoulos, P. S. "A Hybrid Method for Calculating the Inductive Interference Caused by Faulted Power Lines to Nearby Buried Pipelines," *IEEE Transactions on Power Delivery*, Vol. 20, No. 2, April 2005, pp. 1465 – 1473.
- [8] Christoforidis, G. C., Labridis, D. P., Dokopoulos, P. S. "Inductive Interference on Pipelines Buried in Multilayer Soil Due to Magnetic Fields From Nearby Faulted Power Lines," *IEEE Transactions on Electromagnetic Compatibility*, Vol. 47, No. 2, May 2005, pp. 254 – 262.
- [9] Dawalibi, F. P., Southey, R. D., Vukonich, W. "Recent Advanced in the Mitigation of AC Voltages Occurring in Pipelines Located Close to Electric Transmission Lines," *IEEE Transactions on Power Delivery*, Vol. 9, No. 2, April 1994, pp. 1090 – 1097.
- [10] Kopsidas, K., Cotton, I. "Induced Voltages on Long Aerial and Buried Pipelines Due to Transmission Line Transients," *IEEE Transactions on Power Delivery*, Vol. 23, No. 3, July 2008, pp. 1535 – 1543.
- [11] COMSOL Multiphysics [online]. © 2015 [cite May. 30, 2015]. Available online: <http://www.comsol.com>
- [12] Agros2D [online]. © 2015 [cite May. 30, 2015]. Available online: <http://www.agros2d.org/>
- [13] Mathworks [online]. © 2015 [cite May. 30, 2015]. Available online: <http://www.mathworks.com/>
- [14] Governmental regulation 1/2008 Sb. on health protection against non-ionizing radiation.
- [15] ČSN EN 15280 (038369). Evaluation of a.c. corrosion likelihood of buried pipelines – Application to cathodically protected pipelines.